



# Chronic virus infection drives CD8 T cell-mediated thymic destruction and impaired negative selection

Heidi J. Elsaesser<sup>a</sup>, Mahmood Mohtashami<sup>b,c</sup>, Ivan Osokine<sup>d,1</sup>, Laura M. Snell<sup>a</sup>, Cameron R. Cunningham<sup>d</sup>, Giselle M. Boukhaled<sup>a</sup>, Dorian B. McGavern<sup>e</sup>, Juan Carlos Zúñiga-Pflücker<sup>a,b,c</sup>, and David G. Brooks<sup>a,b,2</sup>

<sup>a</sup>Princess Margaret Cancer Center, University Health Network, Toronto, ON M5G 2M9, Canada; <sup>b</sup>Department of Immunology, University of Toronto, Toronto, ON M5S 1A8 Canada; <sup>c</sup>Sunnybrook Research Institute, Toronto, ON M4N 3M5, Canada; <sup>d</sup>Department of Microbiology, Immunology and Molecular Genetics, David Geffen School of Medicine, University of California, Los Angeles, CA 90095; and <sup>e</sup>Viral Immunology and Intravital Imaging Section, National Institute of Neurological Disorders and Stroke, National Institutes of Health, Bethesda, MD 20824

Edited by Rafi Ahmed, Emory University, Atlanta, GA, and approved February 3, 2020 (received for review August 8, 2019)

**Chronic infection provokes alterations in inflammatory and suppressive pathways that potentially affect the function and integrity of multiple tissues, impacting both ongoing immune control and restorative immune therapies. Here we demonstrate that chronic lymphocytic choriomeningitis virus infection rapidly triggers severe thymic depletion, mediated by CD8 T cell-intrinsic type I interferon (IFN) and signal transducer and activator of transcription 2 (Stat2) signaling. Occurring temporal to T cell exhaustion, thymic cellularity reconstituted despite ongoing viral replication, with a rapid secondary thymic depletion following immune restoration by anti-programmed death-ligand 1 (PDL1) blockade. Therapeutic hematopoietic stem cell transplant (HSCT) during chronic infection generated new antiviral CD8 T cells, despite sustained virus replication in the thymus, indicating an impairment in negative selection. Consequently, low amounts of high-affinity self-reactive T cells also escaped the thymus following HSCT during chronic infection. Thus, by altering the stringency and partially impairing negative selection, the host generates new virus-specific T cells to replenish the fight against the chronic infection, but also has the potentially dangerous effect of enabling the escape of self-reactive T cells.**

chronic infection | type I interferon | thymus | immunotherapy | T cell exhaustion

CD8 cytotoxic T lymphocytes (CTL) control viral infections by directly killing infected cells, secreting proinflammatory cytokines, and forming memory cells that protect from viral reexposure. Although most viral infections trigger a potent CTL response that serves to resolve infection, a number of viruses are capable of overcoming this control and establishing a chronic infection. In response to the prolonged viral replication and antigen stimulation (1), the host initiates an immunosuppressive program that actively suppresses antiviral T cell function, leading to CTL exhaustion or physical deletion. Many mechanisms disrupt immunity during chronic infections. In addition to immunosuppressive factors, chronic virus infections such as HIV, hepatitis C virus (HCV), and lymphocytic choriomeningitis virus (LCMV) are also characterized by chronic inflammation that promotes immune exhaustion (2). An emerging understanding is developing that these two seemingly opposing programs are linked and that many of the suppressive mechanisms that inhibit the immune response are mediated as feedback responses to proinflammatory cues (3). We recently identified that type I interferons (IFN-I) lie at the nexus of these two programs, both providing the inflammatory signals necessary to initiate robust immunity, while reciprocally inducing negative regulatory mechanisms that suppress ongoing immune activation (2, 4, 5). Targeting IFN-I signaling during the chronic phase of LCMV infection or HIV infection in humanized mice enhanced antiviral immunity and decreased virus titers (4–7). Thus, throughout chronic virus infections, IFN-I driven inflammation and immunosuppression continually modify and regulate established antiviral

immune responses, although mechanisms through which IFN-I limit long-term T cell responses is not well understood.

The thymus is the central organ for the development and maturation of hematopoietic stem cell (HSC)-derived T cell generation (8). The thymus is critical during early life to produce T cells; however, continued thymopoiesis would also be required in chronic infections to generate new CD8 T cells to balance attrition of exhausted cells. For example, during chronic polyomavirus infection, exhausted CD8 T cell responses are replenished by new virus-specific CD8 T cells emigrating from the thymus and these newly activated cells are critical to sustain antiviral immunity (9, 10). We recently demonstrated that in an established chronic LCMV infection, de novo activated naïve CD8 T cells undergo an altered memory-like molecular differentiation, enabling prolonged functionality and enhanced responsiveness to anti-programmed death-ligand 1 (PDL1) immunotherapy (11). Thus, the generation of new T cells to replenish and augment the existing antiviral responses has critical implications to control chronic viral infections. As a result, emerging techniques are being developed in HSC engineering that aim to generate new T cells to boost the antiviral immune response and alter T cell differentiation to control chronic infections are being developed (12), and all rely on the development of new virus-specific T cells in the thymus. In light of the detrimental role that

## Significance

**There is an intense interest in immune reconstitution and immunotherapy to control and cure chronic infections. Yet, how the fundamental processes that are required to generate new T cells are affected by chronic viruses and how these permutations affect therapeutic reconstitution or underlie adverse disease sequelae are not well understood. We demonstrate that type I interferon signaling directly programs peripheral effector T cells to destroy thymic structure and function, leading to a catastrophic organ depletion. Moderate thymic reconstitution associated with immune exhaustion ultimately occurs, but continued ramifications in the efficacy of hematopoietic stem cell therapy to generate new antiviral T cells and to prevent escape of self-reactive T cells remain long term.**

Author contributions: H.J.E., L.M.S., D.B.M., J.C.Z.-P., and D.G.B. designed research; H.J.E., M.M., I.O., L.M.S., C.R.C., and G.M.B. performed research; H.J.E., M.M., I.O., and D.G.B. analyzed data; D.G.B. wrote the paper; and D.B.M. and J.C.Z.-P. provided intellectual input.

The authors declare no competing interest.

This article is a PNAS Direct Submission.

Published under the PNAS license.

<sup>1</sup>Present address: Department of Laboratory Medicine, University of California, San Francisco, CA 94143.

<sup>2</sup>To whom correspondence may be addressed. Email: dbrooks@uhnresearch.ca.

This article contains supporting information online at <https://www.pnas.org/lookup/suppl/doi:10.1073/pnas.1913776117/-DCSupplemental>.

First published February 24, 2020.

direct IFN-I signaling can have on thymic structure and function (13), it is critical to gain an understanding of how the capacity for therapeutic reconstitution is impacted by an established chronically replicating viral infection.

Diverse pathogens can infect the thymus and many of these pathogens also generate chronic infections, including HIV, LCMV, *Mycobacterium tuberculosis*, and *Toxoplasma gondii* (14–18). In the case of HIV, thymic depletion is evident rapidly after infection with the largest impact being observed in younger patients in which thymopoiesis is more active, but also in adults wherein diminished thymic function is maintained long term (19). Suppression of HIV with antiretroviral therapy increased thymic output (20), suggesting that ongoing viral replication or the factors induced by chronic infection potentiated its atrophy. Herein, we demonstrate that chronic LCMV infection leads to rapid disruption of thymus structure and severe thymocyte depletion. Trafficking of LCMV-specific CD8 T cells to the thymus, killing of infected cells, and resultant destruction of the thymic cortex led to rapid thymocyte depletion and thymic atrophy in chronic but not acute infection. In concert with CD8 T cell exhaustion, thymus cellularity rebounded, although overall cellularity remained depressed. The reinvigoration of exhausted T cells by anti-PDL1 therapy induced a rapid secondary depletion within the thymus and an overall loss of thymic cellularity. Therapeutic HSCT enabled new thymopoiesis and allowed emergence of a small fraction of LCMV-specific T cells that subsequently migrated into the periphery to fight infection. Interestingly, the emergence of new CD8 T cells occurred

despite viral persistence within the thymus, suggesting a breakdown in negative selection. In support of this theory, we demonstrated that small populations of high-affinity, self-reactive T cells could escape thymic selection during chronic infection. Because the stringency of thymic negative selection is reduced during chronic infection, the host is able to generate new virus-specific T cells to fight the pathogen, but also acquires the potentially dangerous side effect of permitting autoreactive T cells to emerge.

## Results

**Chronic LCMV Infection Induces Rapid and Severe Thymic Atrophy.** To address how LCMV infection affects thymic function and T cell generation, we infected mice with acute LCMV-Armstrong (Arm) or chronic LCMV-C113 (C113). Infection with the LCMV-Arm variant induces a robust T cell response that eliminates the infection in 8 to 12 d and leads to protective memory (21). On the other hand, LCMV-C113 generates a chronic infection leading to the expression of host-based regulatory factors and cell populations that suppress antiviral immunity (2). Both LCMV-Arm and C113 efficiently infect the thymus by 5 d after infection, leading to a slight decrease in the frequency of immature CD4/CD8 double positive (DP) thymocytes (Fig. 1 A–C and *SI Appendix, Fig. S1A*). As acute LCMV-Arm infection resolved, LCMV titers became undetectable in the thymus, and the frequency of CD4 and CD8 single positive (SP) and DP thymocytes returned to those observed in uninfected mice (Fig. 1 A–C

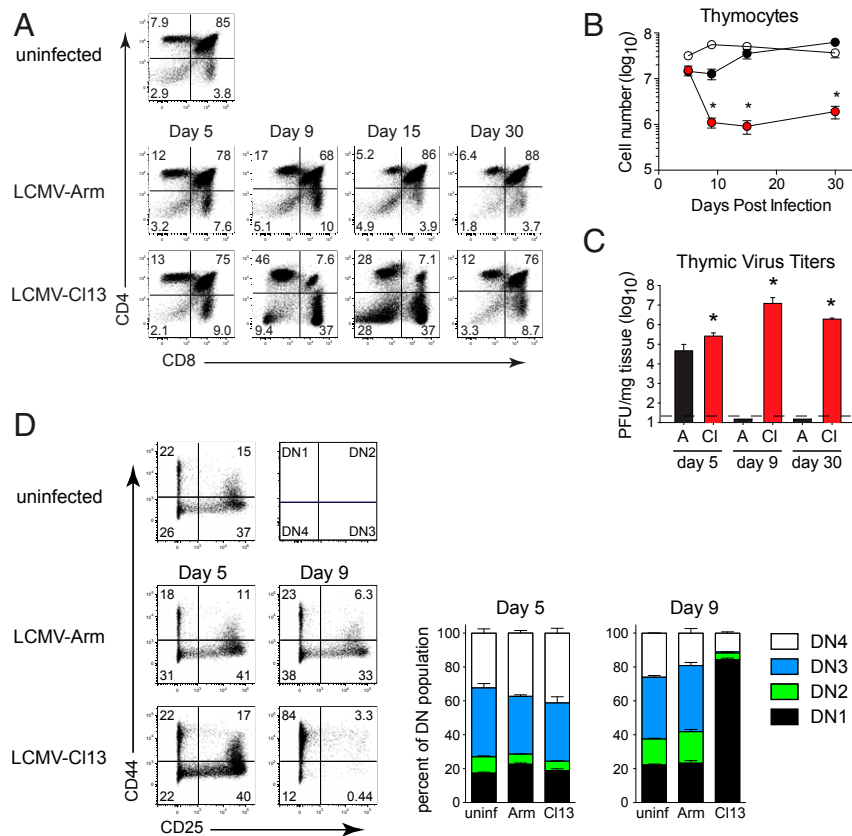


**Fig. 1.** Thymic depletion during chronic LCMV-C113 infection. (A) Mice were infected with LCMV-Arm or LCMV-C113 and euthanized in parallel with uninfected control mice at the indicated day after infection and stained for CD4 and CD8 expression. (B) The total number of thymocytes in uninfected mice (open circles), LCMV-Arm infected mice (black circles), or LCMV-C113 infected mice (red circles). (C) Bar graphs indicate thymus viral titers (plaque-forming units; PFU) at the indicated day in LCMV-Arm (A, black) and LCMV-C113 (CI, red) infected mice. Dotted line indicates the levels of detection. (D) Flow plots and stacked bar graphs indicate the percentage of double negative thymocytes in the DN1, DN2, DN3, and DN4 stages of development in uninfected, or day 5 and day 9 after LCMV-Arm or LCMV-C113 infection. Cells are gated on double negative thymocytes. Data are representative of two to four independent experiments with three to five mice per group. Error bars indicate SD (SD). \* $P < 0.05$ .

and *SI Appendix, Fig. S1A*). On the other hand, virus titers in the thymus remained high during chronic LCMV-C113 infection and promoted near complete depletion of DP thymocytes and a significant decrease in most other thymocyte populations (Fig. 1*A–C* and *SI Appendix, Fig. S1A*). As the chronic infection progressed to day 30, the frequencies of CD4/CD8 SP and DP thymocytes returned to normal relative to naïve mice (Fig. 1*A*). However, the total thymocyte number remained ~10-fold lower than acute LCMV infected or uninfected mice, although the number did increase slightly from the lowest point (Fig. 1*B*). Thus, chronic infection led to a rapid and severe thymic involution that remained numerically depressed for a prolonged period.

To determine whether developmental arrest occurred before the DP stage that affected thymic depletion and reconstitution, we assessed the thymocyte precursor CD4/CD8 double negative (DN) population. We observed that all DN subsets (based on differential CD25 and CD44 expression) exhibited a large decrease in total cellularity following LCMV-C113 infection, with the largest losses occurring from days 5 to 9 within the DN2-4 subsets (Fig. 1*D*). At these time points, the DN1 population represented the majority of total DN cells (Fig. 1*D*). Considering that DP thymocytes require several weeks to transition to this stage (22), their rapid depletion within 3 d (i.e., from day 5 to 8 after LCMV-C113 infection) suggests that a loss of DN thymocytes

does not underlie the depletion of the DP population. DN depletion may instead complicate subsequent T cell reconstitution as the infection progresses. Collectively, these data demonstrate that chronic LCMV infection diminishes thymopoiesis at multiple stages, leading to global and sustained thymic atrophy.

**LCMV Targets Medullary Dendritic Cells within the Thymus.** To better understand the spatial distribution of LCMV within the thymus and gain insights into mechanisms that potentiate rapid thymocyte depletion, we performed immunofluorescence microscopy. Within the thymus, LCMV-C113 infection was predominantly located in the medullary region, which was identified by cytokeratin 5 (CK5) staining (Fig. 2*A*). At day 5, virus antigen was almost entirely restricted to the medullary region and then expanded in distribution by day 9, coinciding with destruction of thymic structure and thymocyte depletion (Fig. 2*A* and *SI Appendix, Fig. S1B*). Thymocytes themselves were only minimally targeted following LCMV-C113 infection (*SI Appendix, Fig. S1C*). Interestingly, a higher proportion of CD45+ versus CD45- cells (i.e., stromal cells) expressed viral antigen, with CD11c+ major histocompatibility complex (MHC) II+ dendritic cells (DC) comprising the majority of LCMV-antigen expressing CD45+ cells (Fig. 2*B*). This high representation of DC among LCMV-antigen-expressing leukocytes was not because the thymus contains a proportionally high number of DC. In fact, CD11c+ MHC II+

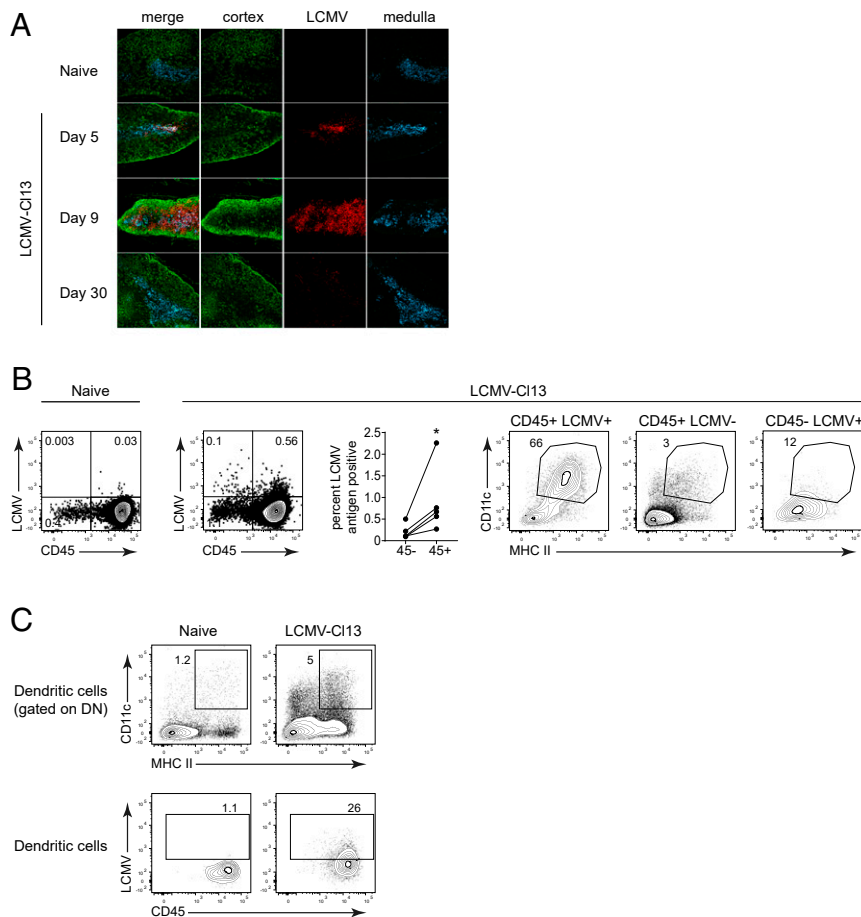


**Fig. 2.** Dendritic cells in the thymic medulla are the primary target of chronic LCMV infection. (A) Immunofluorescence images from naïve and day 8 LCMV-C113 infected thymus. Tissues were stained with anti-LCMV nucleoprotein (red), anti-cytokeratin (CK5; medullary thymic epithelial cells; blue), and anti-CK3 (cortical thymic epithelial cells; green). (B) Naïve and LCMV-C113 infected thymus (day 8) were stained for LCMV nucleoprotein. (Left) LCMV expression in the total CD45 positive and CD45 negative fractions of the thymus. (Right) Frequency of dendritic cells (CD11c+ MHC II+) in the LCMV positive and negative CD45 fractions. (C) Flow plots show the frequency of dendritic cells in the total double negative population (Top) and in the LCMV antigen positive population (Bottom). Data are representative of two to three independent experiments with three to five mice per group. \* $P < 0.05$ .

DC were only minimally represented among uninfected CD45+ cells or infected CD45- cells in the thymus (Fig. 2B). In addition, DC comprised a relatively small proportion of the thymus even when thymocytes were excluded (Fig. 2C). Within the thymic DC population, a high percentage expressed LCMV nucleoprotein (Fig. 2C), suggesting that DC are the primary reservoir of virus within the thymus following chronic LCMV infection.

**The Functional State of Virus-Specific CD8+ T Cells Dictates Thymic Depletion vs Reconstitution.** The rapid and near complete loss of DP thymocytes during chronic LCMV infection led us to next consider an indirect mechanism of deletion. Specific deletion of virus-specific thymocytes via negative selection seemed unlikely given that the majority of thymocytes are not LCMV specific. DP thymocytes are particularly sensitive to glucocorticoid-mediated cell death in other models of infection (23). Glucocorticoids are activated in virus infections and can lead to rapid depletion of DP thymocytes (24). We investigated the role of glucocorticoids in LCMV-induced thymic depletion by using adrenalectomized mice. These mice do not survive beyond day 6 after LCMV-Cl13 infection, but at this time point, thymocyte depletion was evident, and no difference between adrenalectomized and mock-adrenalectomized mice was observed (SI Appendix, Fig. S2A). These data support involvement of a different mechanism underlying thymic destruction in chronic infection.

Peripheral effector CD8+ T cells are capable of homing to the thymus to combat mycobacterial infection (25), and considering the high level of LCMV infection within the thymus, we surmised

that CD8 T cells may target this reservoir of infected cells. To monitor virus-specific CD8 T cell trafficking to the infected thymus, we adoptively transferred naïve LCMV-specific T cell receptor transgenic CD8 P14 T cells (26) (i.e., mature T cells that will otherwise not be present in the recipient) into mice prior to infection. During both acute and chronic infections, virus-specific P14 cells rapidly migrated into the thymus (Fig. 3A). We next determined whether CD8+ T cells mediate thymic depletion by depleting peripheral CD8 T cells prior to infection. Consistent with the reported tissue distribution of depleting antibodies (27), CD8 T cells were depleted from the blood and peripheral lymphoid organs, but not from the thymus, as indicated by the similar profile and amount of thymocytes in uninfected mice treated with isotype vs. anti-CD8 antibody (Fig. 3B). The elimination of peripheral CD8+ T cells prior to LCMV-Cl13 infection almost entirely prevented thymocyte depletion (Fig. 3B), whereas CD4 T cell or natural killer (NK) cell depletion did not (SI Appendix, Fig. S2C). The inability to mediate thymic depletion in the CD8-depleted mice was not due to changes in virus titers within the thymus, which were similar or even slightly increased when CD8 T cells were depleted (SI Appendix, Fig. S2B). To further delineate whether thymic depletion was mediated by virus-specific or bystander CD8+ T cells, we infected mice bearing a transgenic T cell receptor (TCR) recognizing ovalbumin (i.e., OT-1 mice) (28). These mice have CD8 T cells, but do not mount an LCMV-specific CD8 T cell response (29). Similar to CD8 T cell-depleted mice, thymic depletion did not occur in the OT-1 mice following LCMV-Cl13 infection (Fig. 3C), indicating

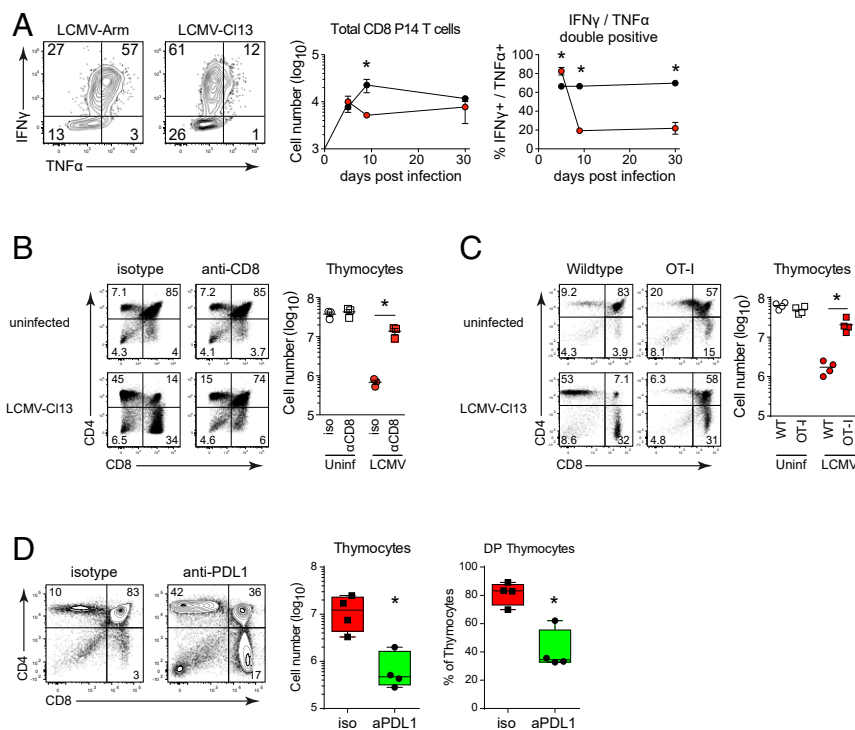


**Fig. 3.** Virus-specific CD8 T cells mediate thymic depletion and their exhaustion in chronic infection enables reconstitution. (A) Mice received LCMV-specific P14 CD8 T cells and were infected with LCMV-Arm or LCMV-Cl13. Flow plots show IFN $\gamma$  and TNF $\alpha$  expression following LCMV-GP<sub>33</sub> peptide stimulation of thymus derived P14 cells. Graphs indicate the number of thymus-infiltrating and the percent of cytokine producing P14 T cells in the thymus on the indicated day following LCMV-Arm (black) or LCMV-Cl13 (red) infection. (B) WT mice were treated with isotype control or anti-CD8 depleting antibody and then either remained uninfected or were infected with LCMV-Cl13 infection 1 day later. Flow plots show thymus depletion and the graph demonstrates total thymic cellularity 9 d after antibody treatment. (C) Thymus depletion and cellularity in uninfected and LCMV-Cl13 infected (day 9) WT and OT-1 transgenic mice. (D) WT mice were treated with isotype control or anti-PDL1 antibody beginning 25 d after LCMV-Cl13 infection. Flow plots show thymocyte profile and graphs indicate total cellularity and the percent of double positive thymocytes. Data are representative of two to three independent experiments with four to five mice per group. Error bars indicate SD. \* $P < 0.05$ .



that virus-specific (not bystander) CD8 T cells mediate thymic depletion during chronic LCMV infection.

We next probed what allowed for reconstitution of thymic populations as chronic infection progressed. Similar to other peripheral tissues, virus-specific CD8<sup>+</sup> T cells infiltrating the thymus were functionally exhausted by day 9 after chronic infection, losing the ability to secrete interferon gamma (IFN $\gamma$ ) and tumor necrosis factor alpha (TNF $\alpha$ ) (Fig. 3A). Interestingly, reconstitution of DP thymocytes coincided with CD8 T cell exhaustion within the thymus, suggesting that attenuation of T cell function during chronic infection might enable thymic reconstitution. To determine the effect of exhaustion on thymic reconstitution and test whether the functionally restored CD8 T cells could deplete the thymus, we treated chronically infected mice with anti-PDL1 blocking antibodies at 25, 28, and 31 d after infection and then the thymus was isolated 2 d after the last treatment. Whereas isotype treatment did not affect thymocyte populations, anti-PDL1 immunotherapy drove rapid depletion of DP thymocytes and loss of cellularity (Fig. 3D). Importantly, thymocyte depletion was not observed in naïve mice, mice that had been previously acutely infected with LCMV-Armstrong, or in OT-1 mice infected with LCMV-Cl13 (*SI Appendix, Fig. S4*). Thus, virus-specific T cell exhaustion enables thymic reconstitution despite viral persistence and the use of immunotherapy during states of thymic infection can reinduce thymus pathology and destruction.

**CD8 T Cell Intrinsic IFNR Signaling Is Required for Thymic Homing and Destruction.** We next sought to uncover the mechanisms underlying CD8 T cell-mediated thymic destruction. IFN-I is an immunomodulatory cytokine produced during numerous bacterial and viral infections that can directly alter thymic stromal cells, thymocyte development, as well as modulate CD8 T cell functions (13). Strikingly, thymocyte depletion following LCMV-Cl13 infection was largely averted in type I IFN receptor knockout (IFNR<sup>-/-</sup>) mice, or in mice treated with anti-IFNR blocking antibodies, compared to wild-type (WT) mice (Fig. 4A and *SI Appendix, Fig. S3A*). Furthermore, whereas total thymic cellularity remained depressed as chronic infection progressed in WT mice, thymocyte numbers returned to preinfection levels by day 30 after infection in IFNR<sup>-/-</sup> mice (Fig. 4A). Restoration was not observed in IFN $\gamma$  receptor knockout (IFN $\gamma$ R<sup>-/-</sup>) or TNF $\alpha$  receptor 1 knockout (TNFR1<sup>-/-</sup>) mice (*SI Appendix, Fig. S2D*). In addition, removal of IFNR signaling from thymic stromal cells using FoxN1-cre x IFNR fl/fl mice also did not prevent thymocyte depletion during chronic infection (*SI Appendix, Fig. S2E*). Collectively, these data demonstrate that thymocyte depletion is IFN-I dependent, but does not rely on signaling in thymic stromal cells.

We next investigated the pathways mediating IFN-I induced thymic depletion. Interferon alpha (IFN $\alpha$ ) and interferon beta (IFN $\beta$ ) bind to the IFNR to activate signal transducer and activator of transcription 1 and 2 (Stat1 and Stat2, respectively) homodimers and heterodimers that induce IFN stimulated gene (ISG) expression in a circuit amplified by interferon regulatory factor 7 (IRF7) activation (3). IFN $\beta$  is associated with enhancing immunosuppression in chronic LCMV infection (30, 31); however, IFN $\beta$  deficiency did not affect thymic depletion (Fig. 4B), indicating that IFN $\alpha$  alone is sufficient to induce T cell targeting of the thymus. Similarly, Stat1 deficiency did not prevent the loss of DP thymocytes or thymic destruction (Fig. 4B). On the other hand, thymic depletion was almost entirely prevented in IRF7<sup>-/-</sup> and Stat2<sup>-/-</sup> mice (Fig. 4B). Importantly, the naïve IFN $\beta$ <sup>-/-</sup>, IRF7<sup>-/-</sup>, Stat1<sup>-/-</sup>, Stat2<sup>-/-</sup>, and WT mice all had similar thymocyte subset distributions and numbers (*SI Appendix, Fig. S3B*), and the frequency and number of LCMV-specific CD8 T cells was unchanged or increased in the knockout mice following LCMV-Cl13 infection (*SI Appendix, Fig. S3C*). These data

indicate that preservation of thymocytes in IRF7 and Stat2-deficient mice is not due to an initial difference in thymus numbers or the failure to generate CD8 T cell responses. Thus, thymic destruction by CD8 T cells is driven by IFN-I, Stat2, and IRF7, but not Stat1.

IFN-I can signal through multiple cell types, all of which could ultimately impact the antiviral CD8 T cell response. To determine whether the requirement for IFNR, IRF7, and Stat2 signaling was CD8 T cell intrinsic, we isolated naïve CD8 T cells from WT, IFNR<sup>-/-</sup>, IRF7<sup>-/-</sup>, or Stat2<sup>-/-</sup> mice and transferred them into OT-1 mice, which due to the lack of virus-specific CD8 T cells, do not themselves exhibit thymic depletion following chronic infection (Fig. 3A). Overall thymic cellularity was slightly (albeit significantly) decreased in all LCMV-Cl13 infected groups compared to uninfected OT-1 mice, even without CD8 T cell transfer (Fig. 5A and B). However, compared to LCMV-Cl13 infected OT-1 mice that received no CD8 T cells, WT CD8 T cells efficiently migrated to the thymus, depleted DP thymocytes and decreased overall thymic cellularity when transferred into OT-1 mice (Fig. 5A–C), further confirming the specific role of CD8 T cells. On the other hand, thymic homing and depletion did not occur in LCMV-Cl13 infected OT-1 mice that received IFNR<sup>-/-</sup> CD8 T cells (Fig. 5A–C), demonstrating direct IFN-I signaling on CD8 T cells is required for thymic depletion. Transfer of Stat2<sup>-/-</sup> CD8 T cells gave a more complex profile with DP depletion and thymic cellularity falling between no transfer and WT CD8 T cell transfer (Fig. 5A–C), suggesting both CD8 T cell intrinsic and extrinsic Stat2 requirements. IRF7<sup>-/-</sup> CD8 T cells effectively mediated thymic destruction the same as WT CD8 T cells (Fig. 5A–C), indicating an indirect effect of IRF7 to drive CD8 T cell function, likely through amplification of IFN-I production by innate immune cells. Interestingly, the amount of thymic depletion was tightly correlated to CD8 T cell infiltration into the thymus (Fig. 5D). Thus, direct IFNR-mediated Stat2 signaling on CD8 T cells in combination with IRF7 signaling by peripheral cells is required for peripheral thymic homing and depletion during chronic infection.

**HSC Transplantation Generates New Virus-Specific CD8<sup>+</sup> T Cells and Autoreactive T Cells in Chronic Infection.** Although thymopoiesis functionally reconstitutes with the induction of T cell exhaustion, the structural and cellular alterations (particularly within the medullary region, which mediates negative selection (32)) may have long-standing consequences on thymic selection and the ability to generate new virus-specific CD8 T cells. A previous study demonstrated that well after chronic LCMV is cleared from most peripheral tissues (including the thymus), newly generated LCMV-specific CD8 T cells can emerge (9). Yet, ongoing viral replication within the thymus should negatively select newly virus-specific CD8 T cells (26). To specifically probe de novo LCMV-specific T cell development during sustained chronic LCMV infection, we generated partial bone marrow chimera mice using the chemotherapeutic agent busulfan (9). Busulfan partially ablates the bone marrow HSC niche without depleting the peripheral immune compartment, allowing for engraftment of donor stem cells without the disruption of the ongoing immune response or a change in virus control (*SI Appendix, Fig. S5A*). Mice were CD4 depleted prior to LCMV-Cl13 infection to generate a life-long viremic infection. Busulfan was administered 30 d after infection and donor HSC provided 1 d later. Donor HSCs introduced into mice efficiently repopulated the peripheral T cell compartment at approximately the same rate and to the same level in uninfected and in chronically infected mice (Fig. 6A), highlighting the functional restoration of thymopoiesis during the established chronic LCMV infection. Donor HSC-derived B cells, which do not require the thymus for development, also repopulated the periphery at a similar, albeit slightly reduced level in LCMV chronically infected mice relative to naïve mice

(Fig. 6A). Surprisingly, despite ongoing viral replication within the thymus, a small percentage of donor (CD45.1+) HSC-derived LCMV-specific CD8 T cells emerged against multiple LCMV-epitopes during chronic infection (Fig. 6B and *SI Appendix, Fig. S5B*), indicating the ability to generate new virus-specific CD8 T cells to replenish the ongoing T cell response, but also suggesting that negative selection is incomplete.

To test whether the diminished efficacy of negative selection was restricted to the generation of virus-specific cells or was a generalized response, we determined whether high-affinity autoreactive T cells could also escape negative selection during chronic infection. Naïve, chronic LCMV-Cl13 infected wild-type mice, or chronic LCMV-Cl13 infected Ova-transgenic (tg) mice that expressed ovalbumin on all cells, were treated with busulfan and given a mix of 80% CD45.2+ HSC from WT mice plus 20% CD45.1+ HSC from OT-1 mice. In this system, OT-1 cells are deleted by negative selection in the thymus of naïve Ova-tg mice,

but not in non-Ova expressing WT mice. As expected, donor-derived OT-1 cells emerged in naïve or chronically infected WT mice and were deleted from naïve OVA-tg mice (Fig. 6C). A slight population of CD45.1+ donor-derived CD8 T cells were present in the naïve Ova-tg mice, but these cells did not express the OT-1 TCR either on the surface or intracellularly (Fig. 6C) and likely arose from rearrangement of endogenous (nontg) TCRs. Interestingly, a small population of OT-1 TCR cells were evident in the spleens in ~40% (3/7 mice) of the chronically infected Ova-tg mice (Fig. 6C and *SI Appendix, Fig. S5C*), with the frequency of OT-1 in these mice ranging from 15 to 75% of transferred CD45.1+ cells. Thus, changes in negative selection stringency have benefits for the continued fight against the persisting pathogen by generating new virus-specific T cells, but the partial impairment can also have the undesired effect of allowing escape of autoreactive T cells.

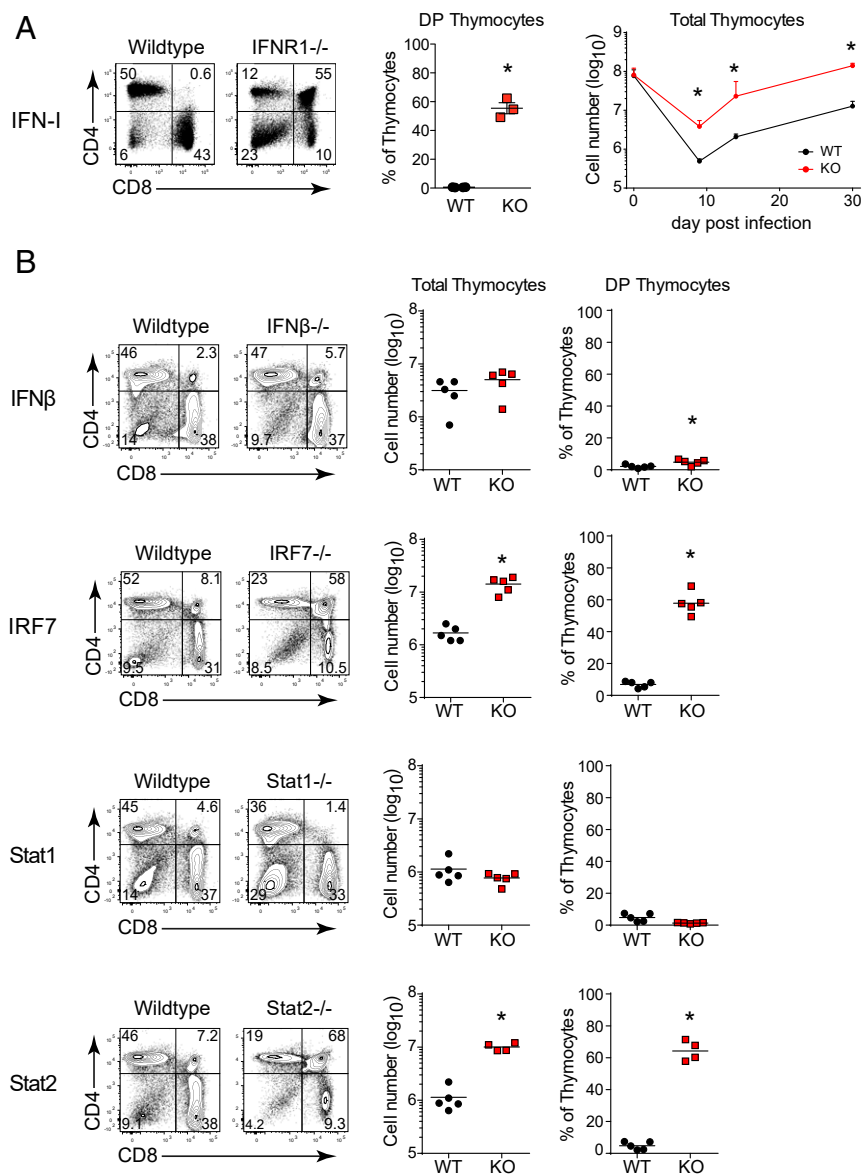


**Fig. 4.** IFN-I in chronic infection drives thymus depletion. (A) Flow plots show the thymus profile, and the bar graphs indicate the percent of double positive thymocytes or of total thymocytes in WT and IFNR<sup>-/-</sup> mice on day 9 after infection. (B) Flow plots show the CD4 vs. CD8 thymus profile and scatter plots the percent of DP thymocytes or total thymic cellularity on day 9 after LCMV-Cl13 infection of WT, IFNβ<sup>-/-</sup>, IRF7<sup>-/-</sup>, Stat1<sup>-/-</sup>, or Stat2<sup>-/-</sup> mice. Data are representative of three to five independent experiments with three to five mice per group. Error bars indicate SD. \*P < 0.05.

## Discussion

The development of T cell-based therapies to supplement or revitalize a dysfunctional antiviral immune response could revolutionize therapies to treat chronic viral infections. As a result, immune reconstitution strategies based on HSC transplantation producing antiviral chimeric antigen receptors or TCRs are moving forward (33). It is therefore critical to understand the short- and long-term consequences of chronic viral infection on the thymus and the ability to generate new T cells. Here, we demonstrate that a chronic viral infection can rapidly target thymic medullary resident DCs, inducing massive thymic destruction and cellular depletion, leaving this lymphoid organ stunted in the DN1 stage of development and markedly reduced in thymocytes. As infection progressed and T cell exhaustion was instituted, thymic function rebounded, allowing for broad restoration of thymocyte subsets and the ability to produce new naïve T cells that augmented the peripheral pool. In addition, the

established chronic infection did not prevent hematopoietic reconstitution by HSCs, and transplantation of naïve cells led to broad spectrum hematopoietic reconstitution of B cells, myeloid cells, and, importantly, T cells. Thus, despite the near complete thymic destruction at the initial stage of chronic viral infection, the thymus is able to regenerate and produce new T cells, despite sustained thymic infection and high systemic levels of inflammation.

Unlike previous mechanisms shown to mediate thymic atrophy during viral infections [e.g., IFN-I-mediated death of thymic stromal cells or glucocorticoid induced depletion of DP thymocytes (8)], we identify a mechanism wherein depletion results from recruitment of and killing by virus-specific CD8 T cells in the thymus. Interestingly, IFN-I production was required for thymic depletion during chronic LCMV infection; however, the effect required IFNR signaling on CD8 T cells rather than thymic stromal cells. This signaling likely enabled the cytotoxic

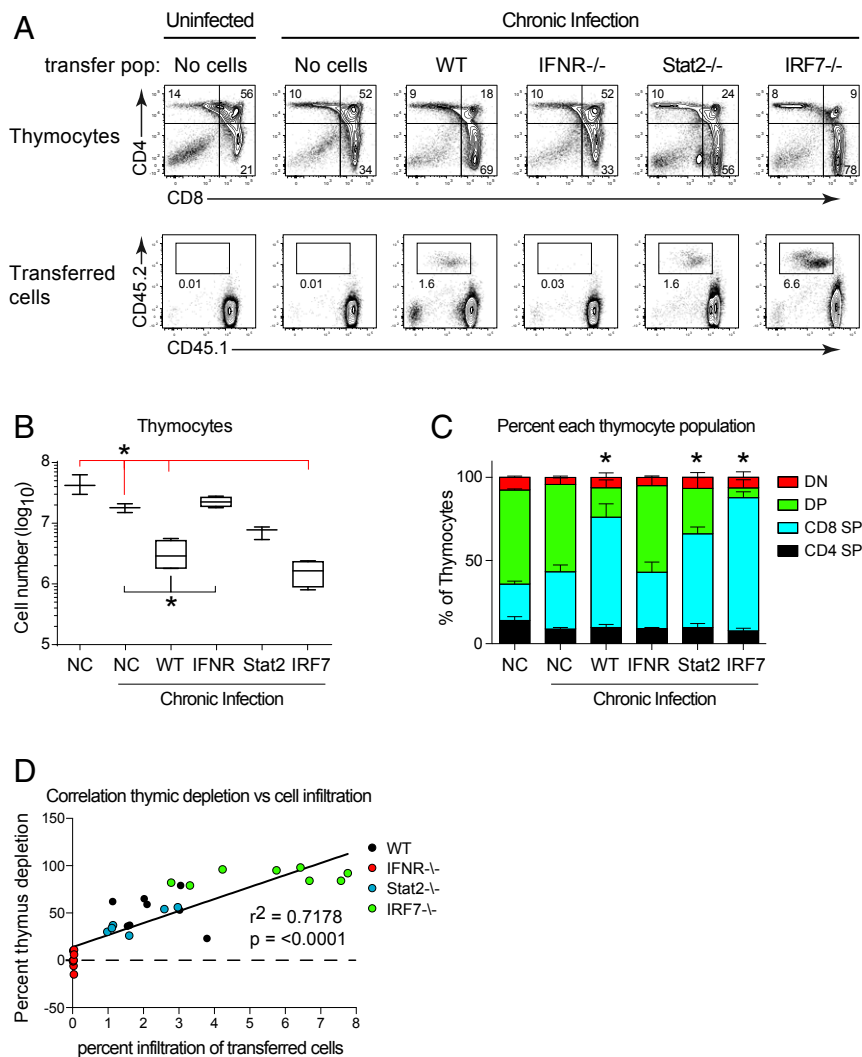


**Fig. 5.** IFNR intrinsic, Stat2-dependent CD8 T cell signaling is required for thymus homing and depletion. OT-1 transgenic mice received no cells (NC) or 2 million purified naïve splenic CD8 T cells from WT, IFNR<sup>-/-</sup>, Stat2<sup>-/-</sup>, or IRF7<sup>-/-</sup> mice. These mice were then either left uninfected (no cells) or infected with LCMV-Cl13. (A, Top) Flow plots represent thymus profile on day 9 after infection. (A, Bottom) Infiltration of transferred CD45.2+ CD8 T cells into the thymus at day 9 after infection. Recipient mice are CD45.1+, CD45.2-. (B) The graph shows thymic cellularity on day 9 after infection. Red \* indicates significance compared to mice that received no cells and were chronically infected. Black \* indicates significance compared to mice that received WT CD8 T cells and were chronically infected.  $P < 0.05$  by one-way ANOVA. Error bars indicated the highest and lowest mouse in the group. (C) Frequency of each thymocyte population in mice receiving CD8 T cells from the indicated strain. Error bars indicate SD. \* $P < 0.05$ . (D) Correlation between the percent depletion of DP thymocytes (y-axis) and the percent infiltration of WT, IFNR<sup>-/-</sup>, Stat2<sup>-/-</sup>, or IRF7<sup>-/-</sup> CD8 T cells into the thymus (x-axis). Data are representative of two to three independent experiments with three to four mice per group.

potential of antiviral CD8 T cells by facilitating their survival and promoting their effector differentiation from the transcription factor T cell factor 1 (TCF1) memory-like population (3, 34, 35). Consistent with this mechanism, mice deficient in CD4 T cells, NK cells, or bearing an irrelevant TCR on their CD8 T cells, all maintain thymic function in the context of high viral replication and associated IFN-I levels. The IFN-I-mediated stimulation of virus-specific CD8 T cells was Stat2 dependent, but Stat1 independent, indicating that Stat2 homodimers or Stat2 heterodimers with other Stat molecules are directly required by the CD8 T cells to mediate thymic pathology. The absence of a role for Stat1 was also consistent with the thymic depletion observed in IFN $\gamma$ -deficient mice. Interestingly, Stat2 appears to mediate both CD8 T cell intrinsic and extrinsic effects of IFN-I during thymic depletion. Moreover, multiple levels of IFN-I amplification were required to license the CD8 T cells, as IRF7-deficient mice (but not CD8 T cells) had reduced thymic destruction. This IRF7 dependency was probably mediated through activation of

the innate immune response and indicates how multiple checkpoints are integrated to regulate the licensing and cellular activation of the CTL response for peripheral homing and killing.

Although the role of IFN-I is well established for maximal virus-specific T cell expansion, survival, and cytolytic effector function, the complex molecular pathways and ISGs that promote these effects are diverse and are yet to be fully characterized (3). IFN-Is directly drive factors required for effector differentiation through STAT signaling, such as CD25, Tbet, GranzymeB and IFN $\gamma$  (35–39). At the onset of chronic viral infection, this results in the promotion of shorter lived GranzymeB+ effector CD8 T cell differentiation at the expense of more long-lived TCF1+ memory-like cells (35). However, they also trigger the expression of ISGs that play key roles in cellular differentiation, survival, and proliferation. IFN regulatory factors (IRFs) are a family of transcription factors that can be up-regulated by IFN-I signaling, guiding short-term responses to proinflammatory signals (IRFs 3, 5, 7, and 9) and cell fate decisions (IRF1, IRF4, and

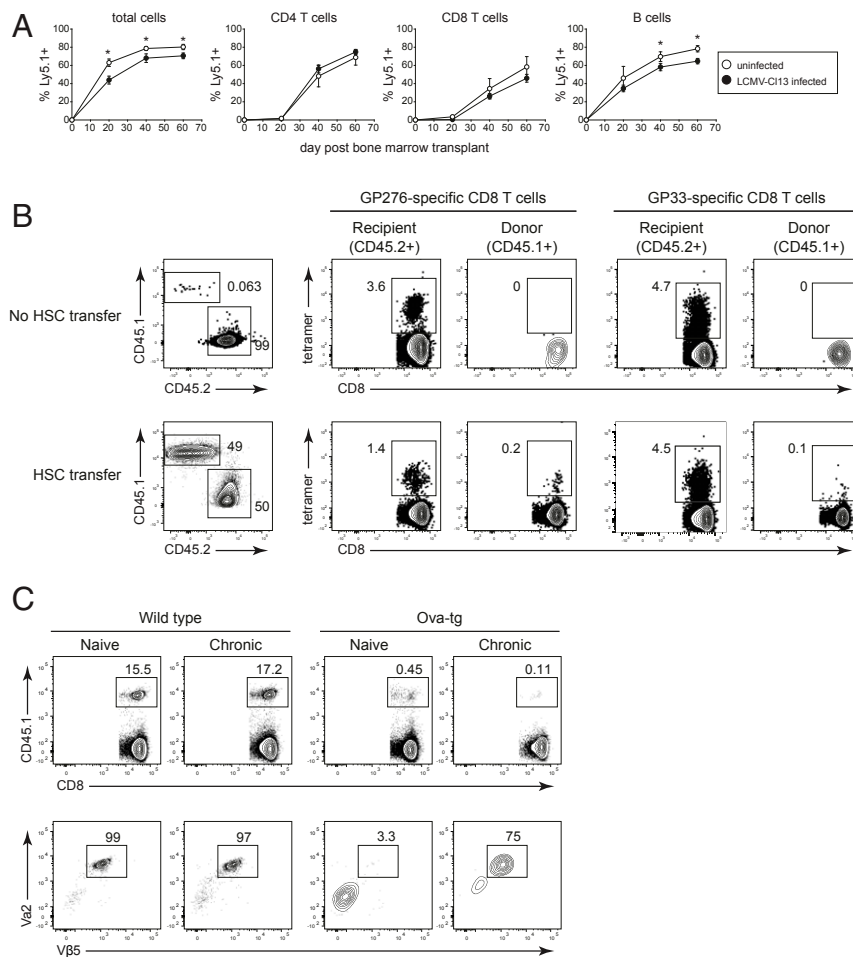


**Fig. 6.** HSC-mediated generation of new LCMV-specific CD8 T cells is accompanied by escape of self-reactive T cells. All mice were CD4 depleted and then either left uninfected or infected with LCMV-Cl13 (generating a life-long viremic infection). All mice then received busulfan and transplant of CD45.1+ HSCs on day 30 after LCMV-Cl13 infection (or after 30 d in the case of the uninfected mice). (A) Donor (CD45.1+) lymphocytes in the peripheral blood of uninfected mice (white circles) or chronically infected mice (black circles) on the indicated day after HSC transplant. (B, Left) Flow plots show the frequency of recipient (CD45.2) and donor (CD45.1) CD8 T cells in the spleen 12 wk after the busulfan treatment and CD45.1+ HSC transplant. In this experiment, some mice received busulfan but not HSC transplant. Flow plots on the right show the frequency of LCMV-GP<sub>276–286</sub> and LCMV-GP<sub>33–41</sub> tetramer staining CD8+ T cells (gated on recipient or donor CD8 T cells). Note, “cells” in the CD45.1 gate in the No HSC transfer group represent background staining from the antibody and serve as a control for the lack of background tetramer staining. (C) Naïve or LCMV- Cl13 infected WT and Ova-transgenic (tg) mice were treated with busulfan and received transplant of 80% WT (CD45.2+) HSC plus 20% OT-1 (CD45.1) HSC. Both naïve mice and mice that were subsequently infected with LCMV-Cl13 were CD4 depleted in parallel at the start of the experiment. (Top) Flow plots show the frequency of OT-1 HSC-derived CD45.1+ cells in the spleen. (Bottom) Flow plots show TCR V $\alpha$ 2 and V $\beta$ 5 staining of the CD45.1+ (OT-1 HSC) donor cells in the spleen. Data are representative of two independent experiments with three to five mice per group. Error bars indicate SD. \* $P < 0.05$ .



IRF8) (38). Additionally, the antiviral ISG, IFITM3 which limits virus entry into host cells, has also been shown to promote the survival of memory CD8 T cells during influenza (40). Further, preferential activation of STAT4 signaling in effectors downstream of IFN-Is promotes effector T cell expansion (41). Thus, rather than a single ISG being responsible for dictating CD8 T cell fate, it is likely that the concerted action of multiple signaling pathways and resultant ISGs act to shape CD8 T cell responses.

Previous work has demonstrated that ongoing thymopoiesis is not necessary to control chronic LCMV infection (42). Our study expands on these findings by demonstrating that chronic infection induces a state of initial functional thymic atrophy, and restoration of thymus function is associated with the virus-specific T cell exhaustion. This is supported by our finding that the initial arrest in T-lymphopoiesis within the thymus is mediated by virus-specific CD8 T cells. As CD8 T cells primed at the onset of infection become functionally exhausted, thymic function and T-lymphopoiesis is restored, demonstrating an additional role for how T cell exhaustion allows normal immune processes to resume during a chronic infection. Thymic recovery as chronic infection progresses is exemplified by our observation that HSCs introduced during chronic infection can seed the bone marrow, reconstitute the thymus, and generate lymphocyte lineages similar to uninfected mice. Interestingly, despite the ongoing chronic virus replication within the thymus, new LCMV-specific T cells were generated, suggesting modification of the stringency of negative selection following the initial thymic destruction. During this new thymic state, high-affinity autoimmune cells that were effectively deleted from naïve animals, were now able to escape negative selection in a subset of mice. The self-reactive T cells were generated at a low frequency but are likely also affected by subsequent peripheral tolerance mechanisms that lead to their functional attenuation or deletion. This could also explain why the virus-specific CD8 T cells were seen in all of the mice tested, whereas self-reactive T cells only emerged in ~40% of mice, since the virus-specific CD8 T cells that emerged would be activated and amplified as opposed to deleted (11). Thus, by altering the stringency of negative selection, the host generates new virus-specific T cells to replenish the fight against the chronic infection, but also has the potentially dangerous side effect of allowing self-reactive T cells to emerge. Since many chronic pathogens can infect the thymus and alter new T cell development, our study has important implications for the design of restorative and immunotherapeutic strategies to rebuild T cell responses and fight chronic infections.

## Materials and Methods

**Mice and Virus.** C57BL/6 (WT) mice were purchased from The Jackson Laboratory or the rodent breeding colony at the Princess Margaret Cancer Center. LCMV-GP<sub>33</sub>-specific CD8 TCR transgenic (P14) mice were bred in-house and have been described previously (43). OT-1 mice (Stock#003831), Ova-transgenic mice (Act-mOVA; Stock#005145), Stat1<sup>-/-</sup> mice (Stock#012606), and Stat2<sup>-/-</sup> mice (Stock# 023309) were purchased from Jackson Laboratory and bred in-house. IFN $\gamma$ R<sup>-/-</sup> mice (Stock#003288), TNFR1 (p55)<sup>-/-</sup> mice (Stock#002818), adrenalectomized mice, and sham adrenalectomized mice were purchased from Jackson Laboratory. IRF7<sup>-/-</sup> mice were provided by the RIKEN BioResource Center. *Irfn*<sup>-/-</sup> (IFN $\beta$ <sup>-/-</sup>) mice were provided by D.B.M., National Institute of Neurological Disorders and Stroke/NIH and bred in-house. IFN $\beta$ <sup>-/-</sup> mice were provided by Eleanor Fish, University of Toronto and bred in-house. All mice were housed under specific pathogen-free conditions. Mouse handling conformed to the experimental protocols approved by the University of California, Los Angeles Animal Research Committee (ARC) and the OCI Animal Care Committee at the Princess Margaret Cancer Center/University Health Network. In all experiments, the mice were infected intravenously (i.v.) via the retro-orbital sinus with  $2 \times 10^6$  plaque-forming units (PFU) of LCMV-Armstrong or LCMV-Clone 13. Virus stocks were prepared and viral titers were quantified as described previously (43).

**Tissue isolation, flow cytometry, and intracellular cytokine stimulation.** Single cell suspensions were prepared from organs and were stained ex vivo using antibodies to CD4 (GK1.5), CD8 (53-6.7), Thy1.1 (H1551), CD45 (30-F11), CD45.1 (A20), CD45.2 (104), MCH II (M5/114.15.2), CD44 (IM7), CD25 (PC61), PD1 (29F.1A12), CD11c (3.9), CD11b (M1/70), and LCMV (VL4). All were from

Biolegend with the exception of Thy1.1 (eBiosciences) and VL4 (BioXcell). For cytokine quantification, splenocytes were restimulated for 5 h at 37 °C with 2  $\mu$ g/mL of MHC class I-restricted LCMV peptide GP<sub>33-40</sub> in the presence of 50 U/mL recombinant murine interleukin-2 and 1 mg/mL brefeldin A (Sigma). Following the 5 h in vitro restimulation, cells were stained with a fixable viability stain, zombie aqua (Biolegend), extracellularly stained as above with CD8, Thy1.1, and fixed, permeabilized (Biolegend cytokine staining kit), and stained with IFN $\gamma$  (XMG1.2) and TNF $\alpha$  (MP6-XT22) (Biolegend). H-2D<sup>b</sup>-restricted LCMV-GP<sub>33-41</sub> tetramer and GP<sub>276-286</sub> tetramer were obtained from the NIH Tetramer core. Samples were run on a FACVerse flow cytometer (BD Biosciences) and data analyzed using Flow Jo software (Treestar).

**Fluorescence microscopy.** Whole thymuses were harvested and fixed in 4% paraformaldehyde (Electron Microscopy Sciences) in phosphate-buffered saline (PBS) overnight at 4 °C prior to incubation with 10% sucrose in PBS gradually increasing the concentration to 30% sucrose over a period of 2 d. Subsequently, the organs were immersed in optimal cutting temperature (OCT) compound (Thermo Fisher Scientific) and snap frozen in liquid nitrogen. Samples were sectioned in the Sunnybrook Research Institute Histology Core Facility using Cryostat Leica CM3050-S. Sections were then either used for treated for hemotoxylin and eosin (H&E) staining or for immunofluorescent microscopy. For immunofluorescence, sections were stained with rabbit anti-cytokeratin 5 (BioLegend), rat anti-LCMV nucleoprotein (Clone VL-4, BioXcell), and mouse anti-cytokeratin 18 (Clone LDK-18, Thermo Fisher Scientific). Secondary antibodies used were anti-rabbit Cy5, anti-rat Rhod Red X, and anti-mouse FITC (Jackson ImmunoResearch Laboratories). Images were taken with a Nikon A1 confocal microscope.

**Isolation and Adoptive Transfer of T Cells.** CD8 T cells were isolated from the spleens of naïve LCMV-specific P14 transgenic mice by negative selection (StemCell Technologies). One thousand P14 cells were injected into naïve mice prior to viral infection. WT, IFN $\beta$ <sup>-/-</sup>, Stat2<sup>-/-</sup>, or IRF7<sup>-/-</sup> CD8 T cells were obtained from the spleens of their respective naïve knockout mice by negative selection. Two million of each population were then transferred into naïve OT-1 mice. All cell transfers were performed i.v. in the retro-orbital sinus.

**Busulfan and Bone Marrow Transfer.** C57BL/6 Ly5.2+ recipient mice were treated i.v. with 500  $\mu$ g anti-CD4 antibody (clone GK1.5; BioXcell) 4 d before infection with  $2 \times 10^6$  PFU LCMV-Cl13. CD4 T cell depletion results in life-long chronic viremic infection. Thirty days after infection, mice were treated intraperitoneally with 30 mg/kg Busulfan (Sigma Aldrich). Bone marrow was harvested from C57BL/6 Ly5.1+ donor mice and depleted of lineage positive cells by negative selection on the autoMACS (Miltenyi Biotec). Lineage-negative cells ( $4.5 \times 10^5$ ) were transferred i.v. into recipient mice 24 h after Busulfan treatment. Mice were given 9 to 12 wk to generate immune cells from donor HSC, upon which mice were euthanized and analyzed. The same strategy was used for the Ova-tg experiments, except that an 80:20 mix of CD45.2+ WT HSC: CD45.1+ OT-1 HSC was used for reconstitution.

**In Vivo Antibody Depletion and Blockade.** To deplete CD8 T cells, CD4 T cells, or NK cells, mice were treated 1 d prior to infection with 250  $\mu$ g anti-CD4 (GK1.5), anti-CD8 (2.43), or anti-NK1.1 (PK136) antibody, respectively. To block IFN-I signaling in vivo during chronic infection, mice were treated i.v. with 500  $\mu$ g anti-IFN $\beta$ 1 blocking antibody (clone MAR1-5A3; Leinco Technologies) or isotype control antibody 1 d before infection and then every 2 d thereafter through day 7, as described previously (44). For PDL1 blockade, mice were administered 250  $\mu$ g of anti-PD-L1 (10F.9G2; BioXcell) or isotype controls at days 25, 28, and 31 of infection and then the thymus was isolated 2 d after the last treatment.

**Statistical Analysis.** Student's *t* tests (two-tailed, unpaired), Mann-Whitney nonparametric tests (two-tailed, unpaired), or one-way ANOVA were performed using GraphPad Prism 5 software (GraphPad Software, Inc.). In all figures, error bars indicate SD.

**Data Availability.** Data, associated protocols, and materials in the paper will be made available to readers upon request to the corresponding author.

**ACKNOWLEDGMENTS.** These researchers are supported by the Canadian Institutes of Health Research (CIHR) Foundation Grant FDN148386 (D.G.B.), NIH grant AI085043 (D.G.B.), an Innovation Grant from the Canadian Cancer Society (CCSR), D.G.B.), the Scotiabank Research Chair (D.G.B.), a training grant from the Fonds de la Recherche en Santé du Québec (L.M.S.), and D.B.M. is supported by the NIH intramural program.

1. L. M. McLane, M. S. Abdel-Hakeem, E. J. Wherry, CD8 T cell exhaustion during chronic viral infection and cancer. *Annu. Rev. Immunol.* **37**, 457–495 (2019).
2. L. M. Snell, D. G. Brooks, New insights into type I interferon and the immunopathogenesis of persistent viral infections. *Curr. Opin. Immunol.* **34**, 91–98 (2015).
3. L. M. Snell, T. L. McGaha, D. G. Brooks, Type I interferon in chronic virus infection and cancer. *Trends Immunol.* **38**, 542–557 (2017).
4. E. B. Wilson *et al.*, Blockade of chronic type I interferon signaling to control persistent LCMV infection. *Science* **340**, 202–207 (2013).
5. J. R. Teijaro *et al.*, Persistent LCMV infection is controlled by blockade of type I interferon signaling. *Science* **340**, 207–211 (2013).
6. A. Zhen *et al.*, Targeting type I interferon-mediated activation restores immune function in chronic HIV infection. *J. Clin. Invest.* **127**, 260–268 (2017).
7. L. Cheng *et al.*, Blocking type I interferon signaling enhances T cell recovery and reduces HIV-1 reservoirs. *J. Clin. Invest.* **127**, 269–279 (2017).
8. D. K. Shah, J. C. Zúñiga-Pflücker, An overview of the intrathymic intricacies of T cell development. *J. Immunol.* **192**, 4017–4023 (2014).
9. V. Zezys *et al.*, Continuous recruitment of naïve T cells contributes to heterogeneity of antiviral CD8 T cells during persistent infection. *J. Exp. Med.* **203**, 2263–2269 (2006).
10. J. J. Wilson *et al.*, CD8 T cells recruited early in mouse polyomavirus infection undergo exhaustion. *J. Immunol.* **188**, 4340–4348 (2012).
11. L. M. Snell, CD8+ T cell priming in established chronic viral infection preferentially directs differentiation of memory-like cells for sustained immunity. *Immunity* **49**, 678–694.e5 (2018).
12. S. G. Kitchen *et al.*, In vivo suppression of HIV by antigen specific T cells derived from engineered hematopoietic stem cells. *PLoS Pathog.* **8**, e1002649 (2012).
13. M. L. Baron *et al.*, TLR ligand-induced type I IFNs affect thymopoiesis. *J. Immunol.* **180**, 7134–7146 (2008).
14. W. Savino, The thymus is a common target organ in infectious diseases. *PLoS Pathog.* **2**, e62 (2006).
15. D. G. Kugler *et al.*, Systemic toxoplasma infection triggers a long-term defect in the generation and function of naïve T lymphocytes. *J. Exp. Med.* **213**, 3041–3056 (2016).
16. C. C. King *et al.*, Viral infection of the thymus. *J. Virol.* **66**, 3155–3160 (1992).
17. W. W. Grody, S. Fligiel, F. Naeim, Thymus involution in the acquired immunodeficiency syndrome. *Am. J. Clin. Pathol.* **84**, 85–95 (1985).
18. H. Pircher, U. H. Rohrer, D. Moskophidis, R. M. Zinkernagel, H. Hengartner, Lower receptor avidity required for thymic clonal deletion than for effector T-cell function. *Nature* **351**, 482–485 (1991).
19. M. L. Dion *et al.*, HIV infection rapidly induces and maintains a substantial suppression of thymocyte proliferation. *Immunity* **21**, 757–768 (2004).
20. D. C. Douek *et al.*, Changes in thymic function with age and during the treatment of HIV infection. *Nature* **396**, 690–695 (1998).
21. R. Ahmed, A. Salmi, L. D. Butler, J. M. Chiller, M. B. Oldstone, Selection of genetic variants of lymphocytic choriomeningitis virus in spleens of persistently infected mice. Role in suppression of cytotoxic T lymphocyte response and viral persistence. *J. Exp. Med.* **160**, 521–540 (1984).
22. Y. Takahama, Journey through the thymus: Stromal guides for T-cell development and selection. *Nat. Rev. Immunol.* **6**, 127–135 (2006).
23. A. L. Gruver, G. D. Sempowski, Cytokines, leptin, and stress-induced thymic atrophy. *J. Leukoc. Biol.* **84**, 915–923 (2008).
24. J. Abramson, G. Anderson, Thymic epithelial cells. *Annu. Rev. Immunol.* **35**, 85–118 (2017).
25. C. Nobrega *et al.*, T cells home to the thymus and control infection. *J. Immunol.* **190**, 1646–1658 (2013).
26. H. Pircher, K. Bürki, R. Lang, H. Hengartner, R. M. Zinkernagel, Tolerance induction in double specific T-cell receptor transgenic mice varies with antigen. *Nature* **342**, 559–561 (1989).
27. G. S. Le Gros, R. L. Prestidge, J. D. Watson, In-vivo modulation of thymus-derived lymphocytes with monoclonal antibodies in mice. I. Effect of anti-Thy-1 antibody on the tissue distribution of lymphocytes. *Immunology* **50**, 537–546 (1983).
28. K. A. Hogquist *et al.*, T cell receptor antagonist peptides induce positive selection. *Cell* **76**, 17–27 (1994).
29. P. Truong, D. B. McGavern, A novel virus carrier state to evaluate immunotherapeutic regimens: regulatory T cells modulate the pathogenicity of antiviral memory cells. *J. Immunol.* **181**, 1161–1169 (2008).
30. C. R. Cunningham *et al.*, Type I and type II interferon coordinately regulate suppressive dendritic cell fate and function during viral persistence. *PLoS Pathog.* **12**, e1005356 (2016).
31. C. T. Ng *et al.*, Blockade of interferon Beta, but not interferon alpha, signaling controls persistent viral infection. *Cell Host Microbe* **17**, 653–661 (2015).
32. T. K. Starr, S. C. Jameson, K. A. Hogquist, Positive and negative selection of T cells. *Annu. Rev. Immunol.* **21**, 139–176 (2003).
33. A. Zhen, M. A. Carrillo, S. G. Kitchen, Chimeric antigen receptor engineered stem cells: A novel HIV therapy. *Immunotherapy* **9**, 401–410 (2017).
34. E. A. Moseman, T. Wu, J. C. de la Torre, P. L. Schwartzberg, D. B. McGavern, Type I interferon suppresses virus-specific B cell responses by modulating CD8+ T cell differentiation. *Sci. Immunol.* **1**, eaah3565 (2016).
35. T. Wu *et al.*, The TCF1-Bcl6 axis counteracts type I interferon to repress exhaustion and maintain T cell stemness. *Sci. Immunol.* **1**, eaai8593 (2016).
36. K. B. Nguyen *et al.*, Critical role for STAT4 activation by type 1 interferons in the interferon-gamma response to viral infection. *Science* **297**, 2063–2066 (2002).
37. M. Wiesel *et al.*, Type-I IFN drives the differentiation of short-lived effector CD8+ T cells in vivo. *Eur. J. Immunol.* **42**, 320–329 (2012).
38. S. Lukhele, G. Boukhaled, D. G. Brooks, Molecular and cellular effects of altered type I interferon signaling in chronic virus infections and cancer. *Semin. Immunol.*, in press.
39. C. Lu *et al.*, Type I interferon suppresses tumor growth through activating the STAT3-granzyme B pathway in tumor-infiltrating cytotoxic T lymphocytes. *J. Immunother. Cancer* **7**, 157 (2019).
40. L. M. Wakim, N. Gupta, J. D. Mintern, J. A. Villadangos, Enhanced survival of lung tissue-resident memory CD8+ T cells during infection with influenza virus due to selective expression of IFITM3. *Nat. Immunol.* **14**, 238–245 (2013).
41. M. P. Gil *et al.*, Regulating type 1 IFN effects in CD8 T cells during viral infections: Changing STAT4 and STAT1 expression for function. *Blood* **120**, 3718–3728 (2012).
42. N. E. Miller, J. R. Bonczyk, Y. Nakayama, M. Suresh, Role of thymic output in regulating CD8 T-cell homeostasis during acute and chronic viral infection. *J. Virol.* **79**, 9419–9429 (2005).
43. D. G. Brooks, D. B. McGavern, M. B. Oldstone, Reprogramming of antiviral T cells prevents inactivation and restores T cell activity during persistent viral infection. *J. Clin. Invest.* **116**, 1675–1685 (2006).
44. I. Osokine *et al.*, Type I interferon suppresses de novo virus-specific CD4 Th1 immunity during an established persistent viral infection. *Proc. Natl. Acad. Sci. U.S.A.* **111**, 7409–7414 (2014).